KU LEUVEN

STADIUS
Center for Dynamical Systems, Signal Processing and Data Analytics

Citation/Reference	Lavanga M., De Wel O., Caicedo A., Heremans E., Jansen K., Dereymaeker A., Naulaers G., Van Huffel S. (2017), **Automatic quiet sleep detection based on multifractality in preterm neonates: effects of maturation.** *Proc. of the 39th Annual International Conference of the IEEE Engineering in Medicine and Biology Society of the IEEE (EMBC 2017)* Jeju Island, South Korea, Jul. 2017, pp. 2010-2013
Archived version	Author manuscript: the content is identical to the content of the published paper, but without the final typesetting by the publisher
Published version	http://ieeexplore.ieee.org/document/8037246/
Journal homepage	http://ieeexplore.ieee.org
Author contact	mlavanga@esat.kuleuven.be +32 16 37 38 28
Abstract	This study investigates the multifractal formalism framework for quiet sleep detection in preterm babies. EEG recordings from 25 healthy preterm infants were used in order to evaluate the performance of multifractal measures for the detection of quiet sleep. Results indicate that multifractal analysis based on wavelet leaders is able to identify quiet sleep epochs, but the classifier performances seem to be highly affected by the infant's age. In particular, from the developed classifiers, the lowest area under the curve (AUC) has been obtained for EEG recordings at very young age (≤ 31 weeks post-menstrual age), and the maximum at full-term age (≥ 37 weeks post-menstrual age). The improvement in classification performances can be due to a change in the multifractality

	properties of neonatal EEG during the maturation of the infant, which makes the EEG sleep stages more distinguishable.
IR	Klik hier als u tekst wilt invoeren.

(article begins on next page)

Automatic quiet sleep detection based on multifractality in preterm neonates: effects of maturation

M Lavanga[1,2], O De Wel[1,2], A Caicedo[1,2], E Heremans[1,2], K Jansen[3,4]
A Dereymaeker[3], G Naulaers[3], S Van Huffel[1,2]

***Abstract*— This study investigates the multifractal formalism framework for quiet sleep detection in preterm babies. EEG recordings from 25 healthy preterm infants were used in order to evaluate the performance of multifractal measures for the detection of quiet sleep. Results indicate that multifractal analysis based on wavelet leaders is able to identify quiet sleep epochs, but the classifier performances seem to be highly affected by the infant's age. In particular, from the developed classifiers, the lowest *area under the curve* (AUC) has been obtained for EEG recordings at very young age (≤ 31 weeks post-menstrual age), and the maximum at full-term age (≥ 37 weeks post-menstrual age). The improvement in classification performances can be due to a change in the multifractality properties of neonatal EEG during the maturation of the infant, which makes the EEG sleep stages more distinguishable.**

I. INTRODUCTION

In recent years, the vast amount of EEG data that have been collected in neonatal intensive care units (NICUs) has made manual sleep scoring extremely time consuming. However, due to advances in biomedical signal processing, automatic neonatal EEG monitoring has become a viable option. Different algorithms to track sleep stages by means of linear and nonlinear EEG features have been published [6]. These methods tend to rely on the fact that quiet or NREM sleep is characterized by a discontinuous tracing, while the active or REM sleep exhibits a more continuous tracing. Among nonlinear features, fractal analysis has received an increased interest to discriminate sleep stages, since it can describe the morphology and the complexity of the EEG signals [1]. In particular, Accardo [1] has shown that the fractal dimension decreases during the slow-wave sleep of full-term newborns, while it reaches its maximum value when the subject is awake. However, the measurement of the fractal dimension investigates only the self-similarity or the global scaling behavior (*long-term persistance*). In contrast, Popivanov [7] has shown that the EEG presents different local scaling behavior, known as multifractality. The fact that the fractal dimension is changing through the different sleep stages highlights the higher complexity of EEG signals compared to a self-similar process like Brownian motion. In addition, the neonatal EEG in the premature infant is in constant development. Especially the duality between the two sleep states evolves during development. Below 31 weeks postmenstrual age (31w PMA) the different sleep stages can not be distinguished, while at 32 to 36 weeks there is a maximal separation between the 2 sleep states. After 37 weeks, different sleep stages start flourishing in the EEG signal with the first seeds of *Tracé Alternant*, which is fully present at full-term age. This study exploits multifractality of neonatal EEG for automatic quiet sleep detection in preterm babies and describes the impact of maturational effects on the performance of this sleep stage classifier.

[1] Department of Electrical Engineering (ESAT), STADIUS Center for Dynamical Systems, Signal Processing and Data Analytics, KU Leuven, Belgium mlavanga at esat.kuleuven.be
[2] imec, Leuven, Belgium
[3]Department of Development and Regeneration, Neonatal Intensive Care Unit, UZ Leuven, Belgium
[4]Department of Development and Regeneration, Child Neurology, UZ Leuven, Belgium

II. METHODS

A. Dataset

Twenty-five preterm neonates, with normal developmental outcome at 2 years, were recruited at the neonatal intensive care unit (NICU) in the University Hospitals Leuven. The patients have a PMA ranging from 27 to 42 weeks. For each subject, eight EEG registrations were recorded according to the restricted 10-20 international system (F_1,F_2,C_3,C_4,T_3,T_4,O_1,O_2) with the electrode C_z as reference. The measurements were performed at least twice during their stay at the unit (at different PMA) and lasted at least 2 hours, producing a dataset of 88 recorded EEGs. The monopolar EEG signals were recorded at a sampling frequency of 250 or 500 Hz. Each channel was filtered using a band-pass filter with a band-pass between 1-20 Hz and subsequently they were downsampled to 128 Hz for uniformity in the analysis. Clinicians manually detected the quiet sleep (QS) and non-quiet sleep epochs (NQS) in the polygraphs, which is required to develop a supervised automated hypnogram. This study mainly investigated QS detection, because the awake states are difficult to discriminate from the active sleep periods at very young age. For this reason, only QS/NQS stages will be referred to in the remaining sections. Figure 1 shows a representative segment for QS and NQS epochs from a recording of a prematurely born neonate at 42w PMA.

B. Multifractal formalism and singularity spectrum

Multifractal signals can be decomposed into different subsets characterized by local Hurst exponents h, which measure the regularities of the signal [4]. Small values of h represent sharp and transient regularity or singularity, while large values represent smooth changes [5]. Similarly to monofractal signals, it is possible to quantify the distribution of the embedding dimensions associated to each value of

h. This function $D(h)$ is called the *singularity spectrum* (SS) and its determination is pivotal to assess the amount of singularities in the signal. A possible way to estimate the SS is multifractal formalism based on wavelet transform modulus maxima. Let $\psi_0(t)$ be a mother wavelet with a positive number of vanishing moments. The discrete wavelet transform (DWT) is defined by the inner product $d_{j,k} = \int_{\mathbb{R}} x(t)\psi_{j,k}(t)dt$, which decomposes $x(t)$ into elementary time-frequency components by means of translation $2^j k$ and dilation 2^j of the mother wavelet [10], since $\{\psi_{j,k}(t) = 2^{-j}\psi_0(2^j t-k), j \in \mathbb{R}, k \in \mathbb{R}\}$. Large scales describe smooth and low frequency oscillations, while small scales describe the sharp transitions in the signal. According to [10] and [7], a partition function $Z(2^j, q)$ can be estimated using the *wavelet leader* $L_f(j,k)$, as follows:

$$Z_L(2^j, q) = \frac{1}{n_k}\sum_{k=1}^{n_k} |L_f(j,k)|^q \sim 2^{j\tau(q)} \tag{1}$$

where $L_f(j,k) \equiv L_\lambda$ represents the maximum wavelet coefficient in the narrow time neighborhood 3λ. Let $\lambda \equiv \lambda_{j,k} \equiv [k2^j, (k+1)2^j)$ be a dyadic interval, such that $d_\lambda = d_f(j,k)$ and let $3\lambda \equiv \lambda_{j,k-1} \cup \lambda_{j,k} \cup \lambda_{j,k+1}$ the union of three dyadic intervals, the wavelet leader is then defined as:

$$L_f(j,k) \equiv L_\lambda = \sup_{\lambda' \subset 3\lambda}\{|d_{\lambda'}|\}, \tag{2}$$

For certain values of q, the scaling exponent $\tau(q)$ (SE) has specific meaning: for positive q, $Z(a,q)$ reflects scaling of large fluctuations, while $Z(a,q)$ reflects scaling of short fluctuations for negative q. In general, for each q, the partition function exhibits a power decay characteristic, such as the power spectrum of 1/f noise. The scaling exponents (SE) associated to this decay can be obtained by computing the slope of Z versus the scales in a log-log diagram. Formally, the function $\tau(q)$ is estimated as follows

$$\tau(q) = \lim_{j\to 0}\inf\left(\frac{log_2(Z_L(2^j,q))}{j}\right) \tag{3}$$

In case of a monofractal signal, $\tau(q)$ is a linear function $\tau(q) = qH - 1$, where H is the global Hurst exponent. In case of a multifractal signal, $\tau(q)$ is a nonlinear function of the local exponents h through the SS, as expressed by $\tau(q) = qh - D(h)$. Indeed, $D(h)$ can be written as the Legendre transform of $\tau(q)$, as follows $D(h) = qh - \tau(q)$ where $h = \frac{d\tau(q)}{dq}$. Since $\tau(q)$ can be decomposed using a Taylor expansion, $\tau(q) = \sum_{p=1}^{\infty} c_p \frac{q^p}{p!}$, SS can be rephrased in terms of the cumulants or coefficients c_p. For this study, we have focused on c_1, c_2 and c_3, which can be associated to the location of the maximum in the SS, the width and the asymmetry of the $D(h)$ distribution, respectively. The width of the SS was also computed as $\Delta h = H_{max} - H_{min}$, where $H_{max} = h(q=-5)$ and $H_{min} = h(q=+5)$. H_{max} and H_{min} represent the Hurst exponents at the extreme right and left of the SS.

C. Quiet sleep detection features

The main hypothesis of this study is that the multifractality features c_1, c_2, c_3 and Δh are able to discriminate QS epochs from NQS periods in neonatal EEG. To evaluate whether this hypothesis is correct, we compared their classification power with the features traditionally used in the literature for this task, as described in [6]. In particular, the power in the main frequency bands, the spectral edge frequency, as well as the spectral moment and the spectral entropy were selected for this subset. Furthermore, Shannon amplitude entropy and fractal dimension (according to Katz's algorithm) were also computed. For each recording, all the mentioned features were computed for 30 s non-overlapping windows in each channel. Each window was labeled as QS or NQS according to the clinicians' labelling. The multifractal features were computed using the Wavelet p-Leader and Bootstrap based MultiFractal analysis (PLBMF) MATLAB toolbox, described in [10]. This toolbox can be downloaded from `https://www.irit.fr/~Herwig.Wendt/software.html`.

D. Classification approach

A feature matrix $\mathbf{X} \in \mathbb{R}^{N\times d}$, where $N = 102209$ and $d = 112$, was produced for the complete dataset. The dimensions of d include 4 multifractal measurements, 9 spectral features and 1 monofractal dimension for each one of the 8 EEG channels ($d = 14*8 = 112$). In addition, each row was associated to a classification vector $\mathbf{Y} \in \mathbb{R}^{N\times 1}$ with 1 for QS and -1 for NQS. In order to develop a supervised model, least-squares SVM [8] have been chosen as a suitable classification method to discriminate QS epochs. To study the maturational effect on QS detection, the dataset $\mathbf{X}$ was first split into three groups according to the infant's PMA. The first group contains all data points that belong to recordings from neonates up to 31 weeks PMA ($N = 11541$). The second one contains all data points from neonates between 31 and 37 weeks PMA ($N = 57053$). The remaining dataset contains all recordings of neonates beyond 37 weeks PMA ($N = 33615$). Despite the splitting, the number of data points is extremely large to train and tune the classification model. In order to reduce the size of the dataset for the training of the classifiers, we used a modified approach to a fixed-size LS-SVM, where a training set with a reduced size M ($M \ll N$) is selected from the available data. In fixed-sized LS-SVM these training points are selected with an iterative process that maximizes the quadratic Renyi entropy. Further details can be found in [3]. However, according to Varon [9] et al., it is possible to choose a reduced size dataset as centroids of M clusters in the original data cloud, which are defined with the k-medoids method. In this way, a dataset with a high entropy can be provided as initial guess for this iterative process [9]. Due to the fact that maximizing the Renyi entropy might lead to the selection of outliers, we reduced the dataset with k-medoids clustering without applying the iterative entropy process, in contrast to [9]. QS classifiers were implemented for the different age groups, as well as for different sets of input features. Specifically, $\mathbf{X}_{katz} \in \mathbb{R}^{N\times 8}$, $\mathbf{X}_{c1,c2,c3} \in \mathbb{R}^{N\times 24}$,

$\mathbf{X}_{\Delta h} \in \mathbb{R}^{N\times 8}$, $\mathbf{X}_{spectral} \in \mathbb{R}^{N\times 72}$, $\mathbf{X}_{c2,\Delta h} \in \mathbb{R}^{N\times 16}$, $\mathbf{X}_{c_2,c_1,c_3,\Delta h,spec} \in \mathbb{R}^{N\times 104}$, $\mathbf{X}_{c_2,c_1,c_3,spec} \in \mathbb{R}^{N\times 96}$, $\mathbf{X}_{all} \in \mathbb{R}^{N\times 112}$ represent the different set of input features used to train the classifiers. The training set was reduced to size $M = 1500$, using the k-medoids method explained before, and the model was tested on the remaining data points for each age group ($N_{test,\leq 31w} = 10041$, $N_{test,\in(31-37)w} = 55553$, $N_{test,\geq 37w} = 32115$). The LS-SVM model was tuned with a 10-fold crossvalidation on the training set. The classifiers' performance was measured as *area under the curve* (AUC) of the ROC curve.

III. Results

Figure 2 depicts the median and the 25 - 75 percentiles for c_2 in QS epochs (dashed line) and NQS ones (continuous line) for the group with the youngest neonates (left panel) and the group with the oldest neonates (right panel). The x-axis in the figures represent each of the EEG channels. The right panel shows that the parameter c_2 discriminates the sleep epochs for the oldest patients (Age $\geq$ 37w PMA) in the channels $[C_3, C_4, O_1, O_2]$, while the left one does not show any discriminative power from c_2 (Age $\leq$ 31w PMA). In Figure 3.a an example of SS for NQS (diamonds) and QS (stars) segments in a recording (prematurely born neonate at 42w PMA) are shown. The latter is wider than the former, leading to the hypothesis that QS has a greater number of singularities, i.e. the QS epochs are more multifractal than the NQS ones. Table I shows the AUC for different LS-SVM classifiers for the different feature sets in the different age groups. Although the spectral features always outperform the fractality measures, it can be seen that the performance of the latter increases with age, especially for the $\mathbf{X}_{c1,c2,c3}$ feature set. This maturation effect is also shown in Figure 3.b, which reports the ROC curves for different age groups using $\mathbf{X}_{c_2,\Delta h}$ as feature set. At the youngest age, the classifier exhibits the lowest performance. Beyond 31w PMA, the AUC dramatically increases reaching its maximum at full-term age. It is interesting to notice that all performance results were obtained with a test set which was at least ten times bigger than the training set (1500 vs 10041, 1500 vs 55553, 1500 vs 32115). In addition, the EEG data were not manually preselected to compute the features.

IV. DISCUSSION

Multifractality seems able to discriminate the QS from the NQS. Although the most known spectral features outperform the multifractal parameters, it should be taken into account that the number of spectral features ($d = 72$) is higher than the number of multifractal moments ($d = 24$) or the Hurst differences ($d = 8$). Furthermore, if the multifractal features are combined with the spectral ones, there is an increase in AUC. Interestingly enough, a marked influence of the age was observed in the performance of the classifiers using the multifractal features, especially when using the input feature set $\mathbf{X}_{c_2,\Delta h}$. The mentioned input set contains features that are related to the width of the SS, which represents the degree of multifractality of the signal (the

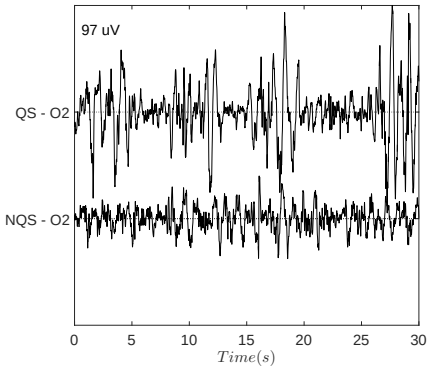
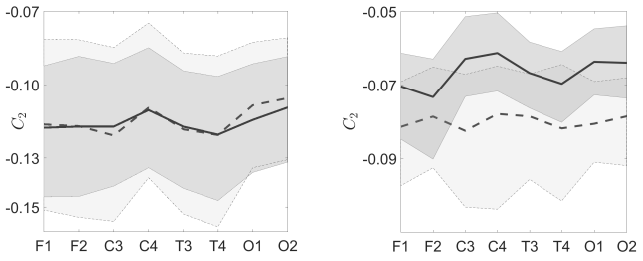
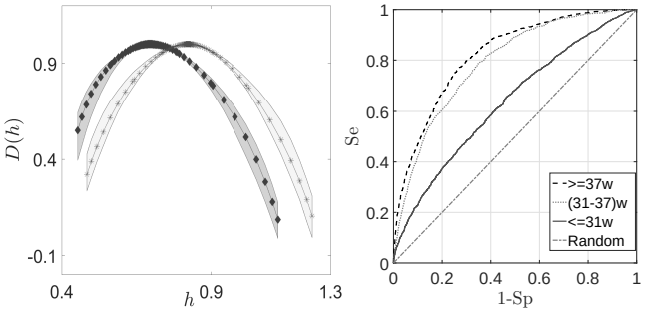


Fig. 1: Example of EEG signal during QS and NQS epoch (prematurely born neonate at 42w PMA).



a) b)

Fig. 2: Median and 25-75 percentile for the c_2 values in QS (dashed line) and NQS (continuous line) epochs. On the left panel, the values from the dataset with the youngest neonates. On the right panel, the values from the dataset with the oldest neonates.



a) b)

Fig. 3: The figure on the left shows an example of a mean singularity spectrum in QS epochs (stars) and NQS epochs (diamonds) for one specific recording (prematurely born neonate at 42w PMA). The figure on the right shows the ROC curve for LS-SVM classifiers, using $\mathbf{X}_{c_2,\Delta h}$ as feature set, in the three different age groups. The continuous line represents the ROC curve for all recordings in the youngest group, the dotted line represents the ROC for all recordings in the middle age group, while the dashed line represents the ROC curve for all recordings in the oldest group.

wider the SS, the more multifractal the signal is). This result indicates that the separation between NQS epochs and the QS epochs based on multifractality in neonatal EEG is more apparent in the oldest group. A possible explanation is that in the youngest premature neonates the discontinuous trace is present both in QS and NQS epochs, while the duality of the two states is well defined above 31w PMA [2]. At full-term age, the trace-alternant replaces QS. These results are in agreement with the clear pattern of fractal dimension changes throughout sleep stages in full-term neonates reported in [1]. Furthermore, Piryatinska [6] showed that the features that better discriminate the sleep stages in preterm neonates are different from the ones in the full-term ones. However, unlike Accardo [1] and Piryantiska [6], we have observed a wider number of Hurst exponents or singularities for QS, which could indicate that the EEG signals are more complex or, at least, characterized by more fractalities or local singularities during QS. However, in the youngest group recordings, the NQS has approximately the same amount of Hurst exponents, as during QS, and they can be regarded as equally complex. In summary, brain maturation has a clear impact on the performances of the classifiers for QS detection in premature neonates, especially when multifractal features are used. This might be caused by the morphological changes in the EEG activity that evolves from a burst-like waveform to a more continuous trace during NQS epochs. These results support the concept that EEG generation mechanisms are highly non-linear.

V. CONCLUSIONS

In this exploratory study, the multifractal formalism, as defined by [10], has been used to analyze neonatal EEG in order to detect QS epochs from NQS epochs in premature infants. Although the multifractal features do not outperform the classical spectral features, they might explain the effect of maturation on the classification performances. This study suggests that the changes in performance can be attributed to the changes in multifractal behavior of the neonatal EEG. In particular, the SS width reduces in NQS compared to QS epochs that makes them easy to classify at age above 32w PMA, which is in agreement to the medical literature [2]. In the light of the above results, new features are required to discriminate QS/NQS over the different postmenstrual ages.

TABLE I: The AUCs for the different LS-SVM classifiers. The rows represent the different input feature sets, while the columns represent the different age groups.

AUC for different classifiers			
Age (PMA w)	≤ 31	$\in (31-37)$	≥ 37
$\mathbf{X}_{Katz}$	.63	.69	.70
$\mathbf{X}_{c_1,c_2,c_3}$	.70	.82	.88
$\mathbf{X}_{\Delta h}$	.67	.78	.79
$\mathbf{X}_{spectral}$	.83	.93	.91
$\mathbf{X}_{c_2,\Delta h}$	.63	.79	.82
$\mathbf{X}_{c_2,c_1,c_3,\Delta h,spec}$	.83	.94	.93
$\mathbf{X}_{c_2,c_1,c_3,spec}$	.84	.93	.93
$\mathbf{X}_{all}$	.82	.94	.92

VI. ACKNOWLEDGEMENTS

This research is supported by Bijzonder Onderzoeksfonds KU Leuven (BOF): The effect of perinatal stress on the later outcome in preterm babies (# C24/15/036); iMinds Medical Information Technologies (SBO- 2016); Belgian Federal Science Policy Office, IUAP # P7/19/ (DYSCO, 'Dynamical systems, control and optimization', 2012-2017); Belgian Foreign Affairs-Development Cooperation (VLIR UOS programs (2013-2019)); ERC Advanced Grant: BIOTENSORS (n° 339804). A.C. is a post-doc fellow at Fonds voor Wetenschappelijk Onderzoek-Vlaanderen (FWO), supported by Flemish government. M.L. is a SB PhD fellow at Fonds voor Wetenschappelijk Onderzoek-Vlaanderen (FWO), supported by Flemish government.

REFERENCES

[1] A. P. Accardo, M. Affinito, M. Carrozzi, S. Cisint, and F. Bouquet, "Comparison between spectral and fractal EEG analyses of sleeping newborns," *Proceedings of the 20th Annual International Conference of the IEEE Engineering in Medicine and Biology Society. Vol.20 Biomedical Engineering Towards the Year 2000 and Beyond (Cat. No.98CH36286)*, vol. 20, no. 3, pp. 1569–1571, 1998. [Online]. Available: http://ieeexplore.ieee.org/lpdocs/epic03/wrapper.htm?arnumber=747191

[2] M. André, M. D. Lamblin, A. M. D'Allest, L. Curzi-Dascalova, F. Moussalli-Salefranque, S. Nguyen The Tich, M. F. Vecchierini-Blineau, F. Wallois, E. Walls-Esquivel, and P. Plouin, "Électroencéphalographie du nouveau-né prématuré et à terme. Aspects maturatifs et glossaire," *Neurophysiologie Clinique*, vol. 40, no. 2, pp. 59–124, 2010.

[3] K. De Brabanter, J. De Brabanter, J. Suykens, and B. De Moor, "Optimized fixed-size kernel models for large data sets," *Computational Statistics & Data Analysis*, vol. 54, no. 6, pp. 1484–1504, 2010.

[4] P. C. Ivanov, L. Amaral, L. Goldberger, S. Havlin, M. G. Rosenblum, Z. R. Struzik, and H. E. Stanley, "Multifractality in human heartbeat dynamics." *Nature*, vol. 399, no. 6735, pp. 461–465, 1999.

[5] R. F. Leonarduzzi, G. Schlotthauer, and M. E. Torres, "Wavelet leader based multifractal analysis of heart rate variability during myocardial ischaemia," in *2010 Annual International Conference of the IEEE Engineering in Medicine and Biology*. IEEE, aug 2010, pp. 110–113. [Online]. Available: http://ieeexplore.ieee.org/document/5626091/

[6] A. Piryatinska, G. Terdik, W. A. Woyczynski, K. A. Loparo, M. S. Scher, and A. Zlotnik, "Automated detection of neonate EEG sleep stages," *Computer Methods and Programs in Biomedicine*, vol. 95, no. 1, pp. 31–46, 2009.

[7] D. Popivanov, V. Stomonyakov, Z. Minchev, S. Jivkova, P. Dojnov, S. Jivkov, E. Christova, and S. Kosev, "Multifractality of decomposed EEG during imaginary and real visual-motor tracking," *Biological Cybernetics*, vol. 94, no. 2, pp. 149–156, 2006.

[8] J. Suykens and J. Vandewalle, "Least Squares Support Vector Machine Classifiers," *Neural Processing Letters*, vol. 9, no. 3, pp. 293–300, 1999. [Online]. Available: http://link.springer.com/10.1023/A:1018628609742

[9] C. Varon, C. Alzate, and J. A. K. Suykens, "Noise Level Estimation for Model Selection in Kernel PCA Denoising," *IEEE Transactions on Neural Networks and Learning Systems*, vol. 26, no. 11, pp. 2650–2663, nov 2015. [Online]. Available: http://ieeexplore.ieee.org/document/7012106/

[10] H. Wendt, P. Abry, and S. Jaffard, "Bootstrap for Multifractal Analysis," *IEEE Signal Processing Magazine*, vol. 24, no. 4, pp. 38–48, 2007. [Online]. Available: http://ieeexplore.ieee.org/xpl/articleDetails.jsp?arnumber=4286563